



Warming-induced cryosphere changes predict drier Andean eco-regions

Amen Al-Yaari, Thomas Condom, Fabien Anthelme, Sophie Cauvy-Fraunié,
Olivier Dangles, Clémentine Junquas, Pierre Moret, Antoine Rabatel

► To cite this version:

Amen Al-Yaari, Thomas Condom, Fabien Anthelme, Sophie Cauvy-Fraunié, Olivier Dangles, et al.. Warming-induced cryosphere changes predict drier Andean eco-regions. *Environmental Research Letters*, 2024, 19 (10), pp.104030. <10.1088/1748-9326/ad6ea6>. <hal-04686152>

HAL Id: hal-04686152

<https://hal.science/hal-04686152v1>

Submitted on 3 Sep 2024

HAL is a multi-disciplinary open access archive for the deposit and dissemination of scientific research documents, whether they are published or not. The documents may come from teaching and research institutions in France or abroad, or from public or private research centers.

L'archive ouverte pluridisciplinaire **HAL**, est destinée au dépôt et à la diffusion de documents scientifiques de niveau recherche, publiés ou non, émanant des établissements d'enseignement et de recherche français ou étrangers, des laboratoires publics ou privés.



Distributed under a Creative Commons CC BY 4.0 - Attribution - International License

LETTER • **OPEN ACCESS**

Warming-induced cryosphere changes predict drier Andean eco-regions

To cite this article: Amen Al-Yaari *et al* 2024 *Environ. Res. Lett.* **19** 104030

View the [article online](#) for updates and enhancements.

You may also like

- [A new data-driven map predicts substantial undocumented peatland areas in Amazonia](#)
Adam Hastie, J Ethan Householder, Eurídice N Honorio Coronado et al.
- [Economics of sustainable irrigation in smallholder agriculture: implications for food security and climate action](#)
Anton Urfels, Alisher Mirzabaev, Stephen Bricx et al.
- [Quantifying the relative contributions of three tropical oceans to the western North Pacific anomalous anticyclone](#)
Zhiyuan Lu, Lu Dong, Fengfei Song et al.

ENVIRONMENTAL RESEARCH
LETTERS

LETTER

OPEN ACCESS

RECEIVED
16 May 2024REVISED
6 August 2024ACCEPTED FOR PUBLICATION
13 August 2024PUBLISHED
30 August 2024

Original content from
this work may be used
under the terms of the
[Creative Commons
Attribution 4.0 licence](#).

Any further distribution
of this work must
maintain attribution to
the author(s) and the title
of the work, journal
citation and DOI.

Warming-induced cryosphere changes predict drier Andean
eco-regionsAmen Al-Yaari^{1,*} , Thomas Condom¹ , Fabien Anthelme², Sophie Cauvy-Fraunié³ , Olivier Dangles^{4,5},
Clémentine Junquas¹, Pierre Moret⁶ and Antoine Rabatel¹ ¹ University Grenoble Alpes, IRD, CNRS, INRAE, Grenoble-INP, Institut des Géosciences de l'Environnement (IGE, UMR 5001), Grenoble, France² AMAP, Univ Montpellier, IRD, CIRAD, CNRS, INRA, Montpellier, France³ INRAE, UR RIVERLY, Centre de Lyon-Villeurbanne, Villeurbanne, France⁴ CEFE, IRD, Univ Montpellier, CNRS, EPHE, Montpellier, France⁵ Pontificia Universidad Católica del Ecuador, Quito, Ecuador⁶ UMR5608 TRACES, CNRS, Université Toulouse Jean-Jaurès, Toulouse, France

* Author to whom any correspondence should be addressed.

E-mail: amen.alyaari@gmail.com**Keywords:** aridity index, snow, Andean eco-regionsSupplementary material for this article is available [online](#)

Abstract

Climate change impacts on humans and ecosystems depend on the intensity, timing, and spatial variability of these changes. While considerable attention has been paid to current and future changes in temperature patterns, comparatively less attention has been devoted to water availability for humans and ecosystems. The aridity index (AI), the ratio of precipitation to potential evapotranspiration, is a common metric used to assess water availability within ecosystems. However, the role of snow in AI calculations within snowy eco-regions is often neglected, resulting in an incomplete understanding of water balance dynamics in these environments. In this study, we estimate aridification under ongoing climate change in Andean eco-regions (AEs), focusing on two horizons: 2050–2060 and 2090–2100. Using monthly TerraClimate data from 2013–2018, we calculated a mean AI for each AE, taking into account the absence of snow (pixels with a snow water equivalent (SWE) < 10 mm/month) and its presence (AI-snow; pixels with a SWE > 10 mm/month). We show that AI allows to differentiate the eco-regions, but that the incorporation of snow in the AI calculation highlights the heterogeneity of aridity conditions within some eco-regions with energy-limited regimes (AI > 1) in the snowy zones and water-limited regimes (AI < 1) elsewhere. Analysis of the CORDEX-SAM regional projections for the periods 2050–2060 and 2090–2100 indicates a general shift towards drier conditions prevailing over wetter conditions in most eco-regions, notably: the Southern Andean Steppe, the Central Andean Wet Puna, the Santa Marta Páramo, and the Peruvian Yungas. The projected reduction in snowfall in CORDEX-SAM, coupled with glacier volume loss, appears to be contributing to the prevalence of aridification across many AEs. These findings highlight potential transitions towards aridification in diverse eco-regions, with repercussions on water availability for humans and ecosystems.

1. Introduction

The South American Andes host a variety of snow-influenced mountain eco-regions (Testolin *et al* 2021), including the high-latitude North-Andean and equatorial páramo, the Peruvian and Bolivian Puna

and the high-latitude Southern Patagonian Andes. More than any other mountain regions, the Andean mountains 'contribute disproportionately to the terrestrial biodiversity' (Rahbek *et al* 2019). In addition, they provide crucial ecosystem services to humanity at both local (e.g. water supply and drinking water,

small-holder agriculture and hydropower) and global levels (e.g. carbon sequestration by high-altitude peat bogs) (Buytaert and De Bièvre 2012, Jacobsen and Dangles 2017). The mountain eco-regions of the Andes are highly vulnerable to land use changes and temperature increases (Grabherr et al 2010, Jacobsen and Dangles 2017), but also to water availability for humans and ecosystems (Bradley et al 2006, Toledo et al 2022). As the cryosphere is shrinking rapidly worldwide, it is essential to understand the consequences of glacier shrinkage and reduced snow cover for humans and ecosystems. The vulnerability of water resources to reduced glacier meltwater and seasonal snow cover has become critical (Bradley et al 2006), with the vast majority of glacierized area in 2020 expected to disappear by the end of the century (Bosson et al 2023).

Given the ecological importance of the Andean eco-regions (AEs) for biodiversity and as nature's contributions to people (Anderson et al 2011) and the sensitivity of their ecosystems to various anthropogenic changes (Sierra-Almeida et al 2010, Anthelme and Lavergne 2018, Cuesta et al 2019), it is essential to characterize the main drivers, especially climatic, and estimate the potential future changes. An accurate quantification of the aridity index (AI; the ratio between precipitation and potential evapotranspiration (PET)) adopted by the United Nations Environment Programme (UNEP 1997), is crucial to assess the vulnerability of terrestrial ecosystems to climate change, especially water stress (Khamis et al 2014). In particular, quantifying the AI is essential for unraveling the complex relationship between precipitation and evapotranspiration within ecosystems, as a valuable tool for assessing water balance and understanding the unique challenges posing any changes in water availability (Berdugo et al 2022). In addition, water availability affects the distribution and composition of terrestrial plant and animal communities as different species adapt to varying moisture levels, nutrient availability, and overall ecosystem functioning (Costantini et al 2016, Hu et al 2018, Zhao et al 2020, Zhang et al 2022). Quantifying the evolution of balance between water availability and potential water loss will thus make it possible to predict changes in the hydrological cycle, which is predicted to become more intense as greenhouse gas emissions increase (Almazroui et al 2021), and shifts in the distribution patterns of organisms. In this way, AI development will make it possible to identify areas at risk of desertification or water scarcity in order to develop effective conservation strategies, and contribute to sustainable management practices in Andean regions (Rockström et al 2009).

AI is usually calculated assuming that the available water is subject to evapotranspiration as reported in the 6th assessment of the IPCC reports (Masson-Delmotte et al 2021) and other global studies (Zomer

et al 2022, Lopes et al 2023, Luo et al 2023, Malpede and Percoco 2023). Within the tropics, snowfalls outside the glacierized area rarely last more than a few days (e.g. Rabatel et al 2013), which has strong consequence on plants and ecosystems (Anthelme and Dangles 2012). In the Andes outside the tropics, the occurrence of snowfalls allows the development of a seasonal snowpack on the ground (e.g. Masiokas et al 2020). In snow-affected AEs, snow cover prevents evaporation and water is not immediately available as it accumulates primarily as snowpack (Hardy et al 2003, Barnett et al 2005). Thus, the presence of snow cover affects the relevance of AI calculations. Therefore, the direct application of the traditional UNEP equation without taking into account for the dynamics of snow cover may lead to imprecise results, especially in the Andean region that experiences varying amounts of snowfall from Ecuador to Patagonia, and more or less prolonged seasonal snow cover.

In this study, we investigate the interplay between water availability, quantified by the AI, and the snow-influenced AEs, taking into account the presence or absence of seasonal snow cover. Our main objective is to identify the nuanced effects of climate change on snow-influenced AEs in the coming decades, with a particular focus on the 2050–2060 and 2090–2100 time frames. Section 2 presents the data sources and methodology used in this study, while section 3 presents the results and ensuing discussion. Finally, the conclusions are presented in section 4.

2. Data and methods

Recent (TerraClimate) and future (CORDEX) climate data, including precipitation, evapotranspiration, and snow cover (validated against reanalysis data), are used to assess the current and future aridity conditions, including snow cover within each Andean ecoregion. The variables available through TerraClimate and CORDEX have slight discrepancies, such as spatial resolution and the distinction between snow water equivalent (SWE; the amount of water contained within the snowpack) and snowfall. Consequently, evaluation and verification are required.

2.1. Climate data

For current climate conditions, we used TerraClimate; a gridded dataset (~4 km) with a global coverage (90° S–90° N, 180° E–180° W) and a monthly temporal resolution that covers the period from 1958 to 2023. It combines the high-spatial resolution climatology of the WorldClim dataset, time-varying Climate Research Unit data (CRU Ts4.0) and the Japanese 55 year Reanalysis (JRA55) (Abatzoglou et al 2018). For our study, we consider monthly precipitation (Pr), PET, and SWE in millimetres per month.

For the future, we used Pr, PET, and snowfall simulated by the South American CORDEX (SA-CORDEX) regional climate models (Giorgi and Gutowski 2015). CORDEX is a global initiative that provides downscaled regional climate projections by utilizing global climate models as input. These downscaled projections provide more detailed and localized information about future climate conditions, taking into account regional-scale climate processes and features (Giorgi and Gutowski 2015). We used CORDEX simulations with a grid resolution of 0.44 degrees at monthly timescales, within the framework of the Coupled Model Intercomparison Project (CMIP5; Taylor *et al* 2012). Although the sixth phase of CMIP is already published (Eyring *et al* 2016, Masson-Delmotte *et al* 2021), their regionally downscaled projections over the Andes are not yet available from CORDEX. Some variables from CMIP6 have been downscaled to 0.25 degrees with daily temporal resolutions (Thrasher *et al* 2022). However, for the calculation of the AI, we need ‘evapotranspiration’, which is not yet available.

The results are based on the mean of available regional models listed in table S1. Each experiment includes one historical simulation (from 1950 to 2005) and three projections (from 2006 to 2100) under three different scenarios. As in Tovar *et al* (2022), in this study, we focus on the worst case scenario (i.e. Representative Concentration Pathways 8.5, RCP8.5) which corresponds to an additional radiative forcing of 8.5 W m^{-2} in the year 2100 relative to the pre-industrial era, without any future environmental and climate change policies.

2.2. Snow and glaciers data

2.2.1. Andean snow water equivalent reanalysis

When considering snow-affected regions, assessing the SWE is crucial for understanding water availability and hydrological processes. The Andean SWE Reanalysis (SWER) dataset, developed by Cortés *et al* (2014) and further expanded by Cortés and Margulis (2017), provides valuable insights into the SWE dynamics in the region of central Chile and Argentina (72°W , 68°W , 38°S , 26°S). This dataset combines direct *in situ* observations, remote sensing data, and modeling techniques to estimate the SWE. It offers high-spatial ($\sim 100 \text{ m}$) and temporal (daily) resolutions over the period from April 1984 to March 2015. We used this observational-based data to evaluate the snow variables of TerraClimate (SWE) and CORDEX simulations (snowfall).

2.2.2. Glacier’s retreat

We used glaciological data (area and volume changes) for all Andean glaciers for the period 2000–2050 from Al-Yaari *et al* (2023). Al-Yaari *et al* (2023)

quantified glacier volume changes through time starting from the glacier outline of the global datasets RGI_V6 (RGI-Consortium 2017) and glacier thickness maps taken from the datasets of Farinotti *et al* (2019) and Millan *et al* (2022), which are representative of the glacier state in the 2000s, and then by applying the corresponding rates of glacier surface elevation changes in an iterative procedure by time steps of 5 years from 2000 to 2050. This methodology is described in detail in Rabatel *et al* (2023). These glaciological datasets allowed us to determine the eco-regions that currently contain glaciers and how these glaciers will change in the future until 2050.

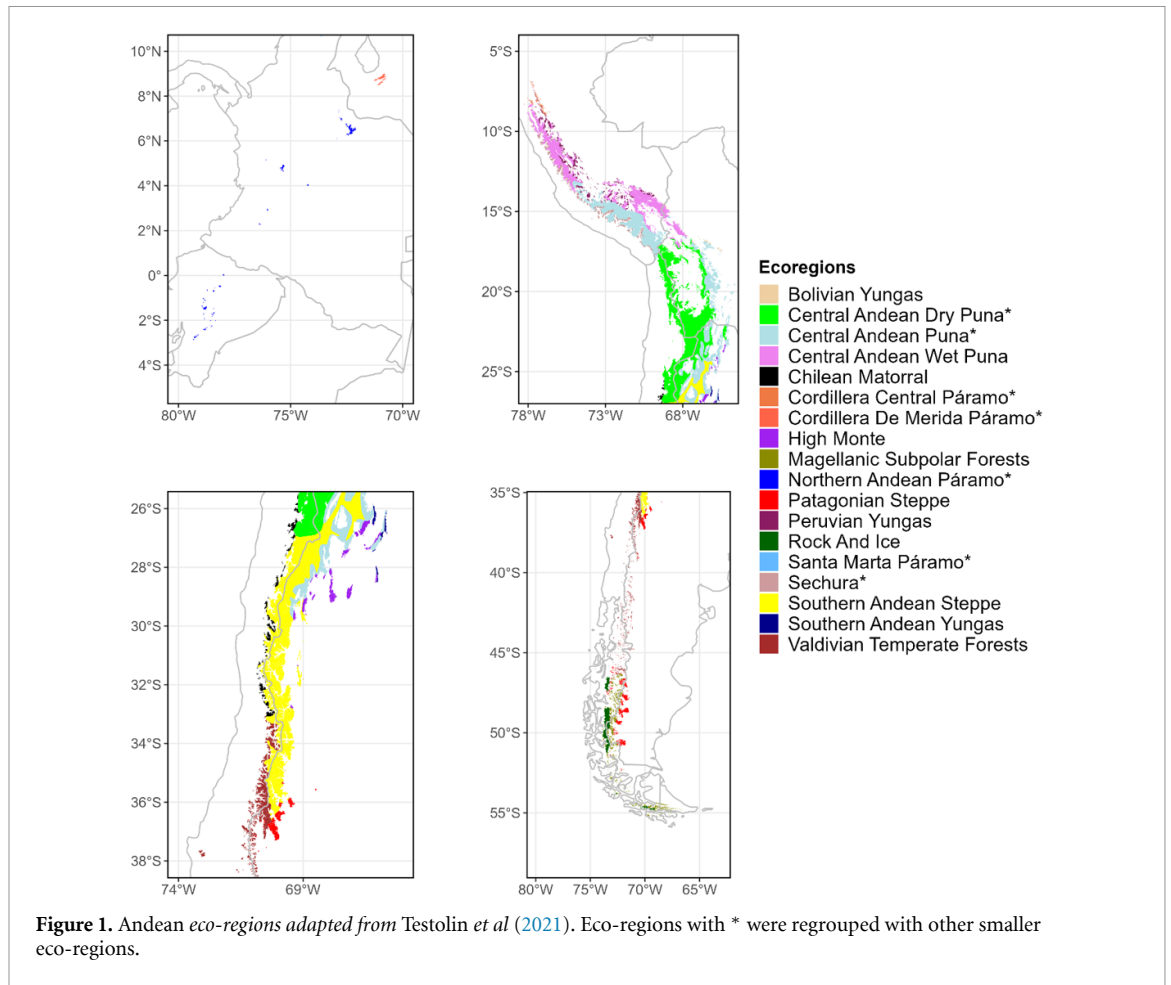
2.3. Present Andean ecosystems, glacier cover and population

We used the map of AEs developed by Testolin *et al* (2021) who identified eco-regions around the globe using a combination of climate datasets, remote sensing products, and biodiversity databases. Testolin *et al* (2021) estimated the global extent of AEs based on empirical data and a high-resolution map of their distribution, using the Google Earth Engine computing platform to select alpine areas within the mountain polygons. Figure 1 shows 18 eco-regions in South America adapted from Testolin *et al* (2021), i.e. an aggregation of small similar eco-regions. The period considered in the analysis of Testolin *et al* (2021) is 2013–2018.

For each eco-region, we calculated the total glacier volume and area in 2010 (table 1). Glaciers with a surface area of less than 0.1 km^2 and more than 100 km^2 have not been considered. Indeed, the future evolution of large glaciers ($>100 \text{ km}^2$), whose response time to changes in climate conditions exceeds several decades, or even centuries, could not be considered with our approach. For the smallest glacier bodies ($<0.1 \text{ km}^2$), the signal-to-noise ratio in the input data (i.e. dh/dt from Hugonnet *et al* (2021) and initial ice thickness distribution from Farinotti *et al* (2019) and Millan *et al* (2022) does not allow an accurate estimate of their future shrinkage. In addition, the approximate population for each eco-region (table 1) was calculated based on Leyk *et al* (2019) and the open-access repository of high-resolution gridded population datasets for Latin America and the Caribbean generated by the interdisciplinary applied research program WorldPop, University of Southampton (McKeen *et al* 2023a, 2023b).

2.4. Evaluation of snow data: TerraClimate SWE and CORDEX snowfall

We used the SWER dataset to conduct a comparative analysis of TerraClimate SWE and CORDEX snowfall simulations for the year 2013. As SWE data is not



available from CORDEX and because SWE and snowfall are not directly comparable, we hypothesized that snowfall should be equal or higher than the SWE at the ground. The comparison is done as follows:

1. SWER data are resampled to the corresponding spatial resolutions of TerraClimate (4 km) and CORDEX (44 km);
2. To evaluate the agreement between TerraClimate SWE data and SWER, we examined TerraClimate monthly SWE by aligning them with the final day of each corresponding month from the daily reanalysis SWER dataset for the year 2013 (see figure S1);
3. For the CORDEX snowfall dataset, we compared the peak in SWE values (maximum annual SWE values) from the SWER data with the simulated annual snowfall values from CORDEX models for the year 2013 (see figure S2).

These comparisons help to identify any discrepancies between the data sets and provide insights into their consistency. SWE, which represents the amount of liquid water that would result from melting the entire snowpack, is related to the amount of snowfall. As snow falls, the thickness of the snowpack

increases, leading to a corresponding increase in SWE. Therefore, we expect the total/year snowfall simulated by CORDEX to exceed the peak/year of SWE values derived from the reanalysis. This serves as an indirect method to assess and validate the accuracy of the CORDEX simulations. We also used the CORDEX snowfall simulations (RCP8.5) to assess the variation in snowfall between the reference period of 2013–2018 and the future periods of 2050–2060 and 2090–2100.

2.5. Computation of the AIs with and without snow for the present time and future

Incorporating SWE estimates is important to obtain a more accurate representation of the water balance and aridity conditions (Sturm *et al* 1995, Pomeroy *et al* 1997). We considered the 2013–2018 period to align with Testolin *et al* (2021), who generated the map of AEs utilized in this study. The periods from 2050 to 2060 (net-zero future) and from 2090 to 2100 (net-negative future) are strategically chosen in alignment with RCPs, which outline different greenhouse gas concentration trajectories and their potential impacts on climate. To compute the AIs with and without snow, we followed these steps:

Table 1. The approximate surface of the Andean eco-regions and the volume and surface-area of glaciers (in the year 2010) within each eco-region. Population is given by McKeen *et al* (2023a, 2023b).

Eco-region identity	Eco-region surface area (km ²)	Glaciers volume ($\times 10^6$ m ³)	Glaciers surface area (km ²)	Population (Number of habitants)
Bolivian Yungas	1 168	230	10	<5 000
Central Andean Dry Puna	1406 699	1 380	47	50 000–500 000
Central Andean Puna	133 650	5 673	192	50 000–500 000
Central Andean Wet Puna	73 218	62 450	1 806	>500 000
Chilean Matorral	4 758	10	0.7	<5 000
Cordillera De Merida Paramo	803	20	0.9	5 000–50 000
High Monte	6 898	54	1.5	<5 000
Magellanic Subpolar Forests	15 180	242 724	4 605	<5 000
Northern Andean Paramo	2,181	6 243	169	5 000–50 000
Patagonian Steppe	12 714	25 565	709	<5 000
Peruvian Yungas	17 207	2 885	119	50 000–500 000
Rock And Ice	11 034	168 458	1 794	0
Santa Marta Paramo	699	474	14	<5 000
Sechura	13 919	242	11	5 000–50 000
Southern Andean Steppe	89 235	85 348	1 839	5 000–50 000
Valdivian Temperate Forests	18 885	52 377	1 397	5 000–50 000
Southern Andean Yungas	1444	—	—	<5 000
Cordillera Central Paramo	2064	—	—	5 000–50 000

1. Separation of non-snowy pixels and snowy pixels for current conditions, using monthly TerraClimate data at a 4 km resolution. For each pixel, if there is at least one month with SWE > 10 mm (indicating snow cover on the ground) over the period [2013–2018], the pixel is classified as a snowy pixel. Otherwise, it is classified as a non-snowy pixel. In addition, if the non-snowy pixel contains a glacier (from RGI_V6), it is considered as a snowy pixel. This process allowed us to calculate the number of snowy and non-snowy pixels for each AE. SWE is used solely to identify and separate pixels and is not included in the formulation for calculating AI or AI-snow.
 2. Calculation of the mean monthly AI and AI-snow (AI with snow, when snow cover occurs on the ground) for the current conditions (2013–2018): We calculated the AI using non-snowy pixels and AI-snow using snowy pixels with monthly TerraClimate data at a resolution of 4 km. The AI and AI-snow time-series are determined as the ratio of P/PET for each pixel and each month. However, for snow pixels, we excluded months where PET equals zero, which typically correspond to the winter months when evapotranspiration is negligible due to snow cover. The mean of the monthly AI and AI-snow values per pixel and per AE was computed over the period 2013–2018. If the mean of AI and AI-snow is smaller (greater) than 1, an eco-region is classified as water-limited (energy-limited).
 3. Calculation of the AI and AI-snow for future conditions (2050–2060 and 2090–2100):
 - 3.1 Aggregation of monthly TerraClimate data (snowy and non-snowy pixels) for the period 2013–2018 from its original 4 km resolution to 44 km resolution, matching the CORDEX dataset. This aggregation applied to both precipitation (liquid + solid) and PET;
 - 3.2 Calculation of the mean values of all monthly, re-sampled to 44 km, TerraClimate precipitation (P) and PET values over the 2013–2018 period, denoted as 'Terr44_current';
 - 3.3 Computation of the mean values of all monthly CORDEX precipitation (liquid + solid) and PET values over the 2013–2018 period, referred to as 'CORDEX44_current'; and
 - 3.4 Division of the CORDEX44_current values by the Terr44_current values to obtain correction matrices. These matrices were then applied to adjust the CORDEX simulations (P and PET) for the entire period from 2013 to 2100. It should be noted that the number of snowy and non-snowy pixels is unchanged for the different periods used in this study.
- Utilizing the adjusted CORDEX dataset under the RCP8.5 scenario, we conducted calculations to determine the average values of AI (and AI-snow) for each AE. Subsequently, k-means clustering was applied to classify these regions into four classes. These classes were defined with the lowest representing arid conditions and the highest representing wet conditions (humid), while the two intermediary classes denote semi-arid and sub-humid conditions.

3. Results and discussion

3.1. Current climate conditions

3.1.1. Evaluation of the TerraClimate SWE vs. the SWER data

Overall, there is a good agreement between the TerraClimate SWE and the SWER data in terms of spatial patterns (see figure S1, which shows the SWE data from TerraClimate and SWER, along with their respective biases, for the year 2013). However, TerraClimate tends to underestimate (or overestimate) the SWE values compared to the reanalysis, which can reach up to 200 mm, over regions between 34°S and 36°S, particularly over the Chilean (or Argentinean) side. This difference may be due to the climate forcing data and the fact that in areas of complex terrain there will be differences due to elevation differences between products. The strength of the leeward effect also appears to be important in capturing the east-west gradient.

3.1.2. Evaluation of the CORDEX snowfall vs. the SWER data

In general, the CORDEX snowfall simulations exhibit higher values compared to the SWER data (see figure S2 for the difference between CORDEX simulations and SWER for the year 2013 over Chile and Argentina), except for a few pixels depicted in yellow (the bias values are mostly higher than 10 mm). This is consistent and confirms our hypothesis.

3.1.3. Aridity conditions of AEs (2013–2018)

Figure 2 presents the AI and AI-snow, of the AEs along the Andes. This figure first shows that the AI values are highly differentiated between the different eco-regions. It also shows that AI values are significantly lower than AI-snow for all eco-regions. Within eco-regions, we observed spatial variability in aridity conditions related to the presence of snow cover. As an example, the snowy zone (pixels) of the Patagonian Steppe is classified as energy-limited (figure 2(b)) using AI-snow, but as water-limited when considering AI (figure 2(a)), indicating a heterogeneity in aridity conditions within an eco-region related to the presence of snow cover. Likewise, in the Peruvian Yungas, there is a spatial variability such that some parts of the eco-region are energy-limited while others lie in the water-limited regime. Similarly, in the Central Andean Wet Puna, which has more coverage (> 4000 pixels), the spatial variability is less pronounced, with almost all pixels lying in the water-limited regime. While the thermal component of microclimatic heterogeneity in high mountains has been carefully studied (see Jacobsen and Dangles 2017, Körner et al 2023, and references therein) and may explain some of this variability, our study suggests that the snow component is also important to

consider when predicting the future of life (including people, ecosystems, and species) in these regions.

3.2. Glaciers, snowfall, and climate projections

In this section, we examine whether the target AEs will experience a reduction in their water resources especially those originating from glaciers and snowfall, in addition to changes in AI.

3.2.1. Glacier's volume change within the eco-regions

Table 2 illustrates the evolution of glacier volume, a critical water resource for downstream areas, within each eco-region between 2000 and 2050. Glacier volume is projected to decrease in all AEs over the coming decades. For instance, in 2050, 75%–100% of the glacier volume present in 2000 is expected to disappear in the Chilean Matorral and Bolivian Yungas eco-regions. Based on the simulated future changes in glacier volume, we can classify the eco-regions into four groups: relatively stable (e.g. High Monte; < 25% loss), moderate loss (e.g. Central Andean Dry Puna, Central Andean Puna, Central Andean Wet Puna, Magellanic Subpolar Forests, Northern Andean Paramo, Patagonian Steppe, Santa Marta Páramo, Southern Andean Steppe, Rock and Ice Neotropics, and Valdivian Temperate Forests; 25%–50% loss), severe loss (e.g. Cordillera de Mérida Páramo, Sechura, Peruvian Yungas; > 50% loss), and total loss (e.g. Chilean Matorral).

3.2.2. Snowfall changes within the eco-regions

Figure 3 illustrates the changes in snowfall estimated for each eco-region between the periods 2013–2018, 2050–2060, and 2090–2100, as derived from the CORDEX simulations. These insights provide a comprehensive view of the evolving snowfall conditions, allowing us to evaluate the changing snowfall patterns within each eco-region. By 2090–2100, snowfall is projected to decrease by at least ~50% across most eco-regions. Particularly noteworthy is the Santa Marta Páramo, which is situated in a region where snowfall is unlikely to occur. This ecoregion is projected to experience a 98% loss over the period 2050–2060, increasing to a 100% loss by 2090–2100. Moreover, eco-regions encompassing the 'Cordillera Central Páramo' are expected to experience a decrease in snowfall by more than 75%, with a 50% reduction already observed over the period 2050–2060.

3.2.3. Present and future aridity conditions in the AEs

The temporal evolution of AI across AEs (figure S3(a)) and AI-snow (figure S3(b)) from 2013 to 2100, based on the RCP8.5 scenario from CORDEX simulations, indicates a declining trend across most eco-regions. For instance, regions like the Bolivian Yungas and the Central Andean Wet Puna display a marked decrease in the AI, suggesting that these areas may

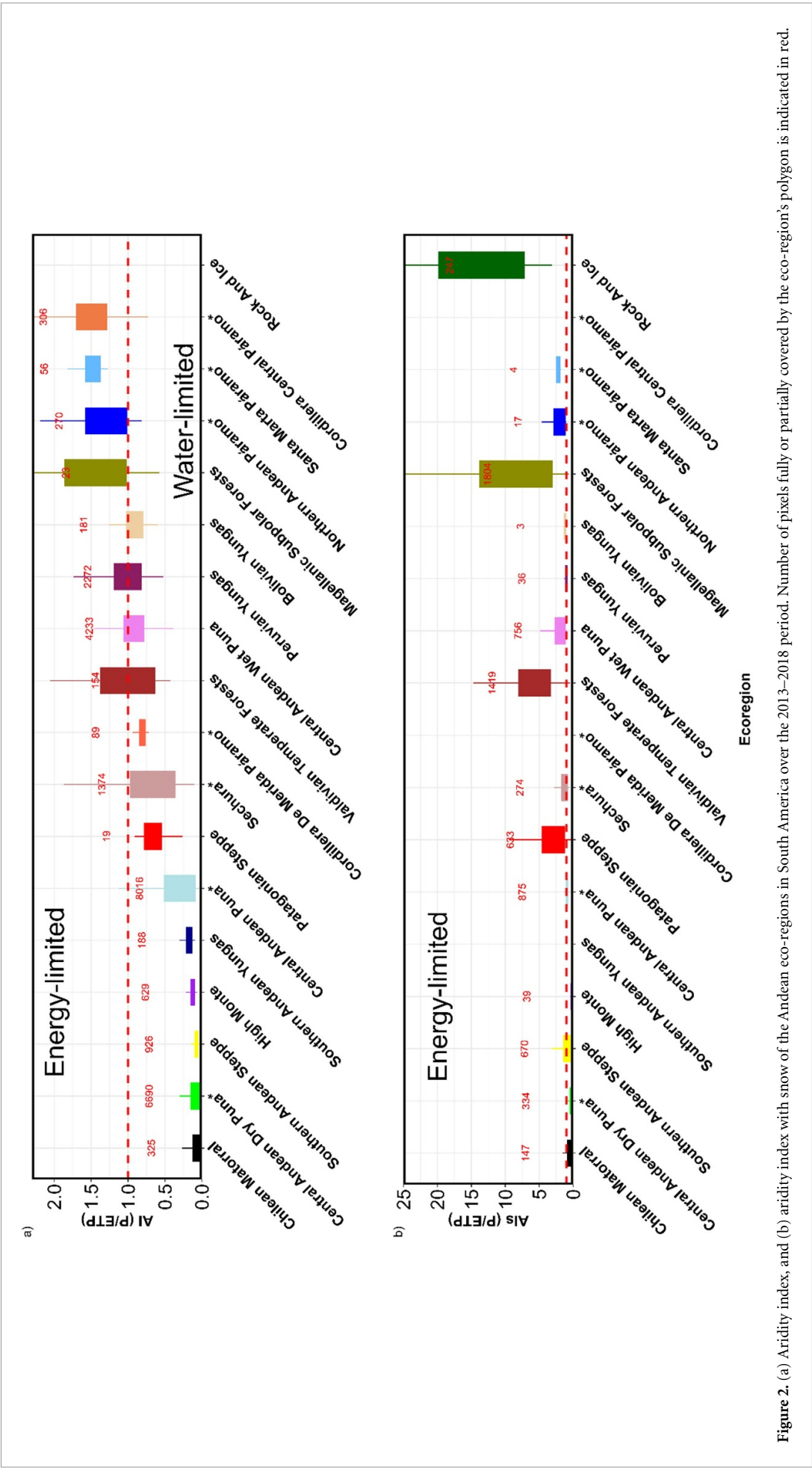
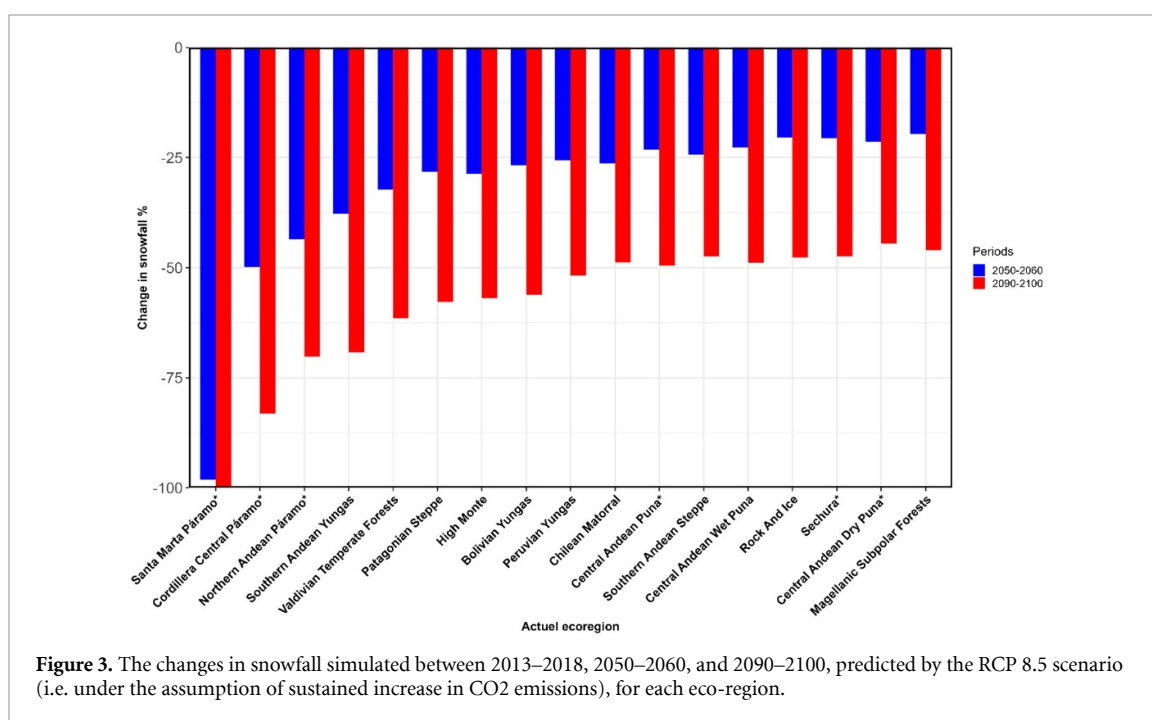


Figure 2. (a) Aridity index, and (b) aridity index with snow of the Andean eco-regions in South America over the 2013–2018 period. Number of pixels fully or partially covered by the eco-region's polygon is indicated in red.

Table 2. Evolution of the glacier volume ($\times 10^6 \text{ m}^3$) within each eco-region between 2000 and 2050.

Eco-region	Volume in 2000 ($\times 10^6 \text{ m}^3$)	Remaining volume in 2050 ($\times 10^6 \text{ m}^3$)	Change from 2000(%)
Bolivian Yungas	285	67	−76
Central Andean Dry Puna	1 189	743	−38
Central Andean Puna	6 944	4 135	−40
Central Andean Wet Puna	70 595	36 705	−48
Chilean Matorral	14	0	−100
Cordillera De Merida Paramo	23	9	−63
High Monte	55	52	−5
Magellanic Subpolar Forests	289 062	187 451	−35
Northern Andean Paramo	6 909	4 114	−40
Patagonian Steppe	28 953	14 651	−49
Peruvian Yungas	3 351	1 600	−52
Rock And Ice	179 825	132 004	−27
Santa Marta Paramo	538	281	−48
Sechura	278	131	−53
Southern Andean Steppe	91 508	63 971	−30
Valdivian Temperate Forests	59 166	29 890	−49



experience more pronounced drying. This trend is observed to varying extents in other regions, such as the Central Andean Puna, Peruvian Yungas, and Northern Andean Páramo, pointing towards a future scenario where increased aridity could lead to significant ecological impacts. This overarching trend of increasing aridity aligns with the expected outcomes under a high-emission scenario, where increased temperatures and altered precipitation patterns contribute to reduced water availability and heightened evaporation, thus stressing the ecosystems in these biomes. Our results suggest an increase in aridification

(i.e. precipitation is projected to decrease and evaporation to increase) in most eco-regions, which can lead to worsening drought and water deficits by 2100. Even if future trends of precipitation show large uncertainties, the trend in the snowfall will necessarily decrease due to the significant increase in temperatures in future projections (Tovar *et al* 2022).

Aridity conditions and their changes, for the periods 2013–2018 and 2090–2100, are shown as alluvial plots in figures 4(a) (AI) and (b) (AI-snow). Similar figures for the period 2050–2060 are provided in the supplementary materials (figures S4(a) and (b)).

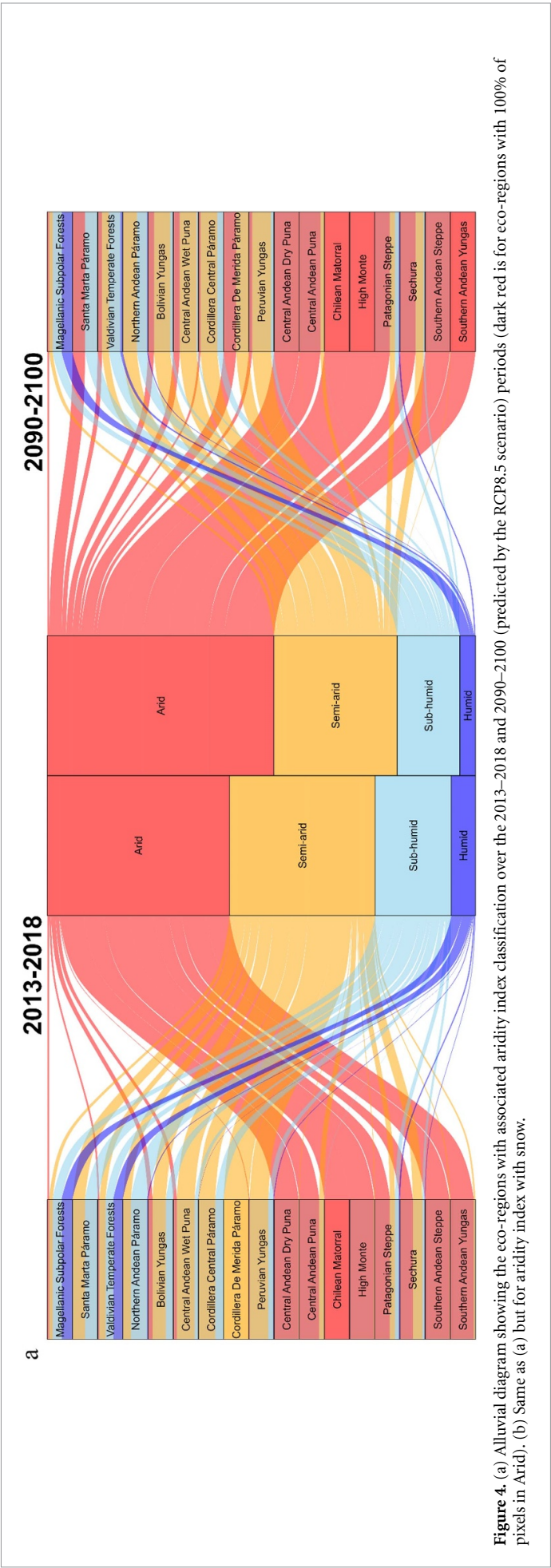
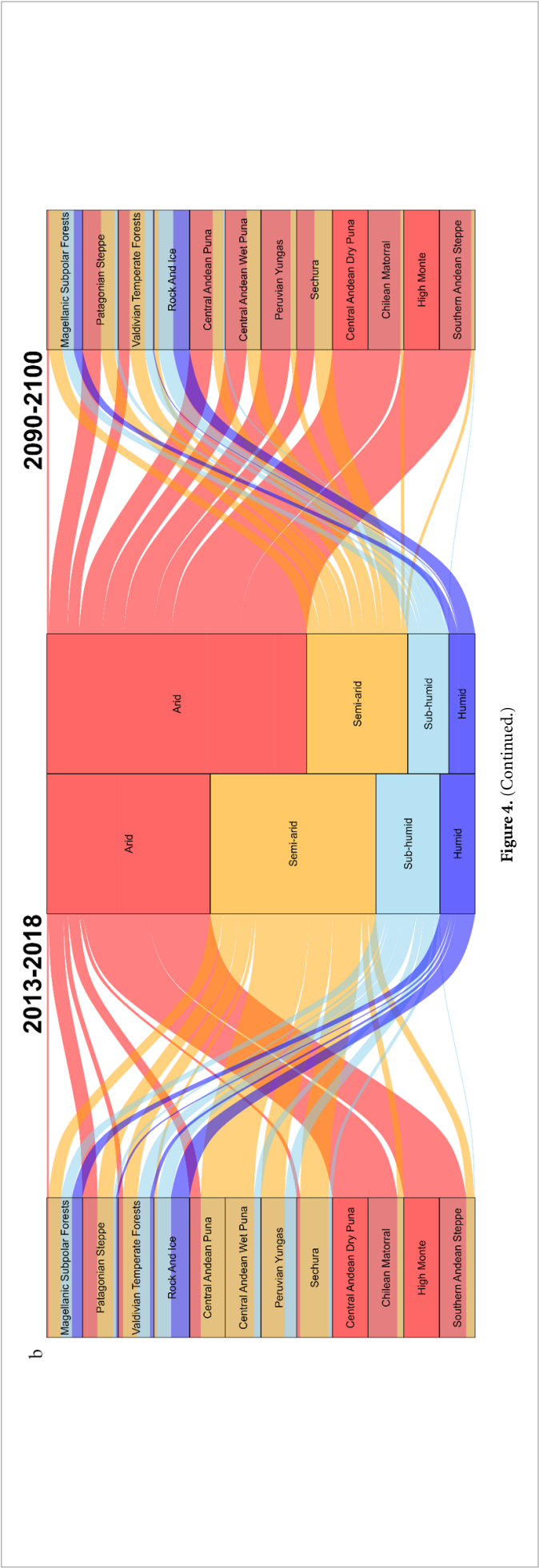


Figure 4. (a) Alluvial diagram showing the eco-regions with associated aridity index classification over the 2013–2018 and 2090–2100 (predicted by the RCP8.5 scenario) periods (dark red is for eco-regions with 100% of pixels in Arid). (b) Same as (a) but for aridity index with snow.



Overall, our analysis shows a predominance of aridification in most eco-regions. Specifically, when considering AI, the semi-arid class is projected to be completely supplanted (replaced by the arid class) in the Southern Andean Yungas and Santa Marta Páramo eco-regions. Tovar *et al* (2022) indicated that grasslands/steppes in the Central and Southern Andes are expected to experience the most significant reductions in suitable climatic conditions for the maintenance of current ecosystems. In 2100 in the Cordillera de Merida Páramo, half of the semi-arid class is expected to be predominantly replaced by the arid class. Bolivian Yungas are located where sub-humid zones are projected to shift from 30% to 12%, while semi-arid areas are anticipated to increase from 52% to 65% (figure S5(a)). The humid class is likely to vanish in the Peruvian Yungas, where arid regions are poised to increase from 3% to 10%, with sub-humid regions experiencing a decrease from 19% to 10% (figure S5(a)). The humid class in the Central Andean Wet Puna, most populated ecoregion ($> 500\,000$), is projected to disappear by 2100 in the non-snowy zones (figure S5(a)). In this eco-region, arid classes will emerge in the snowy zones, replacing the sub-humid zones (figure S5(b)). The absence of snowfall, as mentioned in the previous section over Santa Marta Páramo and Cordillera Central Páramo could explain the prevalence of the arid class in these areas.

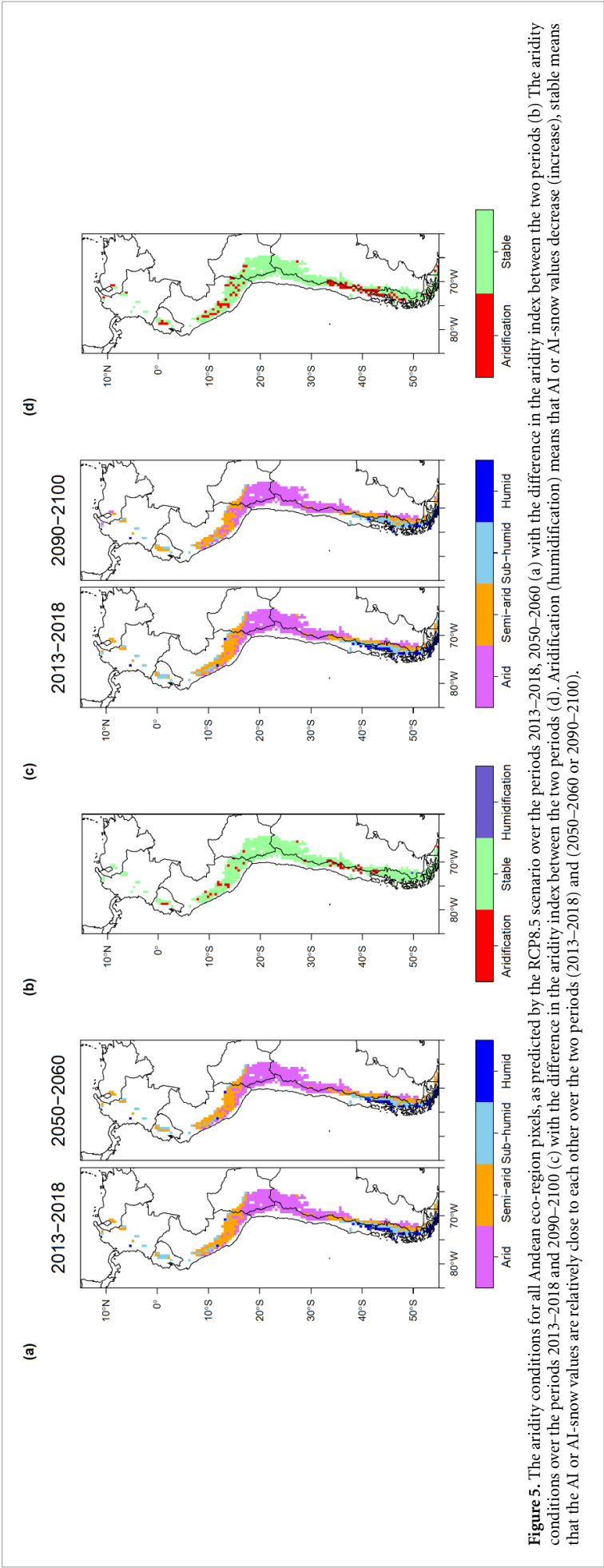
We observe a stronger projected prevalence of the arid class when considering AI-snow over the snowy zones within eco-regions (figure 4(b)) compared to non-snowy zones (figure 4(a)). Refer to figures S5(a)–(d) for the percentage changes between the period 2013–2018 and the projected periods 2050–2060 and 2090–2100 for each class. In the Peruvian Yungas in 2090–2100, for instance, both the sub-humid (33%) and semi-arid (66%) classes in 2013–2018 will be largely replaced by the arid class (83%) and only 17% is likely to remain as semi-arid, which is more severe than when considering AI. The arid class is poised to entirely replace the sub-humid class in the Central Andean Wet Puna. This could also be related to topography (Tovar *et al* 2022, Gutierrez *et al* 2024) as warming is generally projected to be stronger at higher (pixels with AI-snow) than at lower elevations (pixels with only AI). In future studies, incorporating higher-resolution data such as the NASA/GDDP CMIP6 (Thrasher *et al* 2022), would enhance our understanding of localized climate impacts. These findings emphasize the potential shifts to more arid conditions and the dominance of arid classes in various eco-regions particularly when seasonal snowpacks are present, which can have implications for the ecosystems and water availability for people in these regions. Some researchers propose a connection between biomass production of the

vegetation in mountain ecosystems and the presence of unusual snow events, as indicated by studies such as those conducted by Otto *et al* (2011) and Anderson *et al* (2021).

For snowy eco-regions, we employ a similar formulation to the standard AI. However, we exclude months where PET equals zero, typically corresponding to the winter months when evapotranspiration is negligible due to snow cover. Nonetheless, some remaining months with very low evapotranspiration values may still be included in the calculation, which could explain why the humid region in figure 4(b) appears larger than that in figure 4(a). These small evapotranspiration values can influence the AI-snow, making it appear less arid than it actually is during certain periods.

The spatial changes in the aridity of the AEs between the periods 2013–2018, 2050–2060, and 2090–2100 are depicted in figure 5. The aridification is expected to occur (in red) mainly in latitudes between 10° S and 20° S and between 32° S and 45° S, making local populations more vulnerable. A recent study by Aranda *et al* (2023) has already reported snow cover area reductions at low elevations and middle elevations for spring (34 km^2) and summer (86.5 km^2) in the Yeso River basin (located in the semi-arid Andes of central Chile; 33.6° S– 70.0° W) using the snow product (MOD10A2) from the Moderate Resolution Imaging Spectroradiometer. The eco-regions in latitudes between 20° S and 30° S and around 50° S are likely to experience lower levels of aridification and will be more stable. The extent of aridification within the studied AEs is projected to be 12% in the year 2050 and anticipated to reach 17% by the decade 2090–2100, impacting a population of $\sim 5\,000\,000$ and $\sim 8\,000\,000$ (current estimate) inhabitants, respectively.

These results confirm the findings of Tovar *et al* (2022) that the AEs are expected to undergo significant transformations due to the profound impacts of climate change on their biophysical limits (e.g. the total available water supply, the loss of meltwater from glaciers and snowpack, etc). Among others, these changes could have particularly harmful consequences for the little-known biodiversity of the Santa Marta Páramo, which is probably developing the highest endemism of all the Andes (Anthelme *et al* 2014). Similarly, the Southern Andean Yungas and Peruvian Yungas, with their position at a major biogeographical crossroads and their azonal climate, have developed an exceptional biodiversity (Moraes and Sarmiento 2018). Predicting strong aridification in this ecoregion would thus be a consistent threat to an exceptional biodiversity in the next decades. In both cases, the effects of aridification could combine with the effects of glacial retreat to increase



the negative impact of changes on local biodiversity (Anthelme *et al* 2022). The expected strong aridification of the Central Andean Wet Puna, on the other hand, would affect a densely populated area (more than 500 000 people; table 1), most of which rely on nature's contributions to people (Madriral-Martínez and Miralles 2019). It could therefore have far-reaching consequences for the standard of living, health and well-being of Andean inhabitants here and in downstream areas.

The differences in the AI observed between the current period (2013–2018) and future periods (2050–2060 and 2090–2100) are influenced by a combination of natural factors and human activities, and the interactions between these drivers are indeed complex. Natural climate variability, including phenomena such as El Niño and La Niña, can significantly impact precipitation patterns and temperatures. These variations can lead to changes in evapotranspiration rates (Moura *et al* 2019) and overall aridity. Beyond short-term variability, long-term trends such as global warming contribute to changes in temperature and precipitation patterns. This can result in shifts in the hydrological cycle, impacting both water availability and demand. The CORDEX projections used in our study incorporate different greenhouse gas emission scenarios. Increased emissions lead to higher global temperatures, which in turn influence regional climate patterns. The scenarios reflect varying levels of mitigation efforts and their potential impacts on future climate conditions. Determining the relative contributions of natural factors and human activities to changes in AI is inherently complex due to the interactions between these drivers. Future research should continue to explore these interactions to refine our understanding and improve projections of aridity under various climate scenarios.

4. Conclusion

In this study, we assessed the aridity status under current climatic conditions using TerraClimate data and projected future changes using the CORDEX projections. A key aspect of our investigation was to analyze how the inclusion of snow in the AI calculations can affect the results, especially in relation to the SWE threshold used to differentiate pixels with an SWE > 10 mm (AI-snow) from those with an SWE < 10 mm (AI). First, we found that AI, in general, can serve as a useful tool for characterizing eco-regions based on their aridity levels, providing valuable information for ecological studies. Second, the AI values were considerably lower than AI-snow values for all eco-regions, affecting both zones with water and energy limited regimes within eco-regions. This suggests that considering snow in the calculation of the AI is crucial for an accurate assessment

of water availability within eco-regions. Thirdly, several key points regarding the aridity conditions in the AEs based on the CORDEX projections spanning two periods: 2050–2060 and 2090–2100, are observed. The outcomes uncover a prevailing tendency of arid categories replacing wetter classifications across the majority of AEs. The projected lack of snowfall in specific regions (Santa Marta Páramo and Cordillera Central Páramo) may explain the future prevalence of the arid class in these areas. The extent to which this aridification is significant requires further research.

All the glaciers studied within the AEs are experiencing a reduction in their volumes. By the year 2050, glaciers within the Chilean Matorral and Bolivian Yungas eco-regions are likely to experience the most rapid declines, with a loss of approximately 75%–100% of their glacier volumes between 2000 and 2050. This trend may indicate that these eco-regions are particularly sensitive to the effects of global warming. The decline in glacier volume is poised to be exacerbated by projected shifts in aridity patterns across various eco-regions, as predicted through AI classifications. Aridification is more pronounced when considering the AI-snow, with a higher increase in arid areas compared to eco-regions without snow. Regions between latitudes 10° S and 20° S and 35° S and 45° S are expected to experience increased aridification, potentially increasing the vulnerability of already vulnerable populations more susceptible to the negative impacts of these changes. Specific eco-regions, such as the Central Andean Wet Puna (the most populated among all the eco-regions studied), are highlighted for potential shifts in aridity conditions, with the humid classification expected to disappear and the arid classification projected to increase.

In summary, the study suggests a trend towards aridification in AEs, with potential implications for ecosystems, water availability, and the vulnerability of populations in specific latitudinal ranges. The findings highlight the importance of considering snow-related factors and adjusting the AI calculation in regions affected by snow. A more accurate assessment of water availability can be achieved by incorporating snowpack dynamics and considering snowmelt processes. Future research and assessments should consider the influence of snow accumulation and melting processes on water availability by further investigating the impact of different SWE thresholds on the calculation of the AI. This may help to develop or refine more sophisticated methodologies that take snow-related factors into account in AI calculations. There are certainly other factors (the evolution of groundwater, population trends, and various activities including industrial and agricultural practices) that influence water availability in densely populated areas, which should be studied further. Achieving transformative adaptation for mountain water security deserves a focused

and evidence-based transdisciplinary collaboration involving science, policy, and local communities (Drenkhan et al 2023).

Data availability statement

TerraClimate data can be freely downloaded from www.climatologylab.org/terraclimate-variables.html. The Andean Snow Water Equivalent Reanalysis are publicly available at <https://margulis-group.github.io/data/>. The CORDEX simulations are publicly available on the Earth System Grid Federation (ESGF; <https://esg-dn1.nsl.liu.se/search/esgf-liu/>), after creating an account. This is done by clicking the Create Account link in the top right of the provided link.

All data that support the findings of this study are included within the article (and any supplementary files).

Acknowledgments

This study is part of the project Life Without Ice, funded by the BNP Paribas Foundation. The funder had no role in the study design, data collection and analysis, decision to publish or preparation of the manuscript. This study is also conducted as part of the International Research Network (IRN) ANDES-C2H, a joint initiative of the IRD and universities and institutions in Colombia, Bolivia, Peru, Ecuador, Chile, and Argentina. Most of the computations presented in this paper were performed using the GRICAD infrastructure (<https://gricad.univ-grenoble-alpes.fr/calcul.html>) which is supported by Grenoble research communities. People from IGE acknowledge the support of LabEx OSUG@2020 (*Investissements d'avenir*—ANR10 LABX56).

ORCID iDs

Amen Al-Yaari  <https://orcid.org/0000-0001-7530-6088>

Thomas Condom  <https://orcid.org/0000-0002-4408-8580>

Sophie Cauvy-Fraunié  <https://orcid.org/0000-0001-8600-0519>

Antoine Rabatel  <https://orcid.org/0000-0002-5304-1055>

References

- Abatzoglou J T, Dobrowski S Z, Parks S A and Hegewisch K C 2018 TerraClimate, a high-resolution global dataset of monthly climate and climatic water balance from 1958–2015 *Sci. Data* **5** 170191
- Al-Yaari A, Condom T, Junquas C, Rabatel A, Ramseyer V, Sicart J-E, Masiokas M, Cauvy-Fraunié S and Dangles O 2023 Climate variability and glacier evolution at selected sites across the world: past trends and future projections *Earth's Future* **11** e2023EF003618
- Almazroui M et al 2021 Assessment of CMIP6 performance and projected temperature and precipitation changes over South America *Earth Syst. Environ.* **5** 155–83
- Anderson E P et al 2011 Consequences of climate change for ecosystems and ecosystem services in the tropical Andes *Climate Change and Biodiversity in the Tropical Andes* vol 1 (Inter-American Institute of Global Change Research (IAI)) pp 1–18
- Anderson T G, Christie D A, Chávez R O, Olea M and Anchukaitis K J 2021 Spatiotemporal peatland productivity and climate relationships across the Western South American Altiplano *J. Geophys. Res. Biogeosci.* **126** e2020JG005994
- Anthelme F, Carrasquer I, Ceballos J L and Peyre G 2022 Novel plant communities after glacial retreat in Colombia: (many) losses and (few) gains *Alp. Bot.* **132** 211–22
- Anthelme F and Dangles O 2012 Plant–plant interactions in tropical alpine environments *Perspect. Plant Ecol. Evol. Syst.* **14** 363–72
- Anthelme F, Jacobsen D, Macek P, Meneses R I, Moret P, Beck S and Dangles O 2014 Biodiversity patterns and continental insularity in the Tropical High Andes *Arct. Antarct. Alp. Res.* **46** 811–28
- Anthelme F and Lavergne S 2018 Alpine and arctic plant communities: a worldwide perspective *Perspect. Plant Ecol. Evol. Syst.* **30** 1–5
- Aranda F, Medina D, Castro L, Ossandón Á, Ovalle R, Flores R P and Bolaño-Ortiz T R 2023 Snow persistence and snow line elevation trends in a Snowmelt-Driven Basin in the Central Andes and their correlations with hydroclimatic variables *Remote Sens.* **15** 5556
- Barnett T P, Adam J C and Lettenmaier D P 2005 Potential impacts of a warming climate on water availability in snow-dominated regions *Nature* **438** 303–9
- Berdugo M, Vidiella B, Solé R V and Maestre F T 2022 Ecological mechanisms underlying aridity thresholds in global drylands *Funct. Ecol.* **36** 4–23
- Bosson J B, Huss M, Cauvy-Fraunié S, Clément J C, Costes G, Fischer M, Poulénard J and Arthaud F 2023 Future emergence of new ecosystems caused by glacial retreat *Nature* **620** 562–9
- Bradley R S, Vuille M, Diaz H F and Vergara W 2006 Threats to water supplies in the Tropical Andes *Science* **312** 1755–6
- Buytaert W and De Bièvre B 2012 Water for cities: the impact of climate change and demographic growth in the tropical Andes *Water Resour. Res.* **48**
- Cortés G, Giroto M and Margulis S A 2014 Analysis of sub-pixel snow and ice extent over the extratropical Andes using spectral unmixing of historical Landsat imagery *Remote Sens. Environ.* **141** 64–78
- Cortés G and Margulis S 2017 Impacts of El Niño and La Niña on interannual snow accumulation in the Andes: results from a high-resolution 31 year reanalysis *Geophys. Res. Lett.* **44** 6859–67
- Costantini E A C, Branquinho C, Nunes A, Schwilch G, Stavi I, Valdecantos A and Zucca C 2016 Soil indicators to assess the effectiveness of restoration strategies in dryland ecosystems *Solid Earth* **7** 397–414
- Cuesta F, Llambí L D, Huggel C, Drenkhan F, Gosling W D, Muriel P, Jaramillo R and Tovar C 2019 New land in the Neotropics: a review of biotic community, ecosystem, and landscape transformations in the face of climate and glacier change *Reg. Environ. Change* **19** 1623–42
- Drenkhan F, Buytaert W, Mackay J D, Barrand N E, Hannah D M and Huggel C 2023 Looking beyond glaciers to understand mountain water security *Nat. Sustain.* **6** 130–8
- Eyring V, Bony S, Meehl G A, Senior C A, Stevens B, Stouffer R J and Taylor K E 2016 Overview of the coupled model intercomparison project phase 6 (CMIP6) experimental design and organization *Geosci. Model Dev.* **9** 1937–58
- Farinotti D, Huss M, Fürst J J, Landmann J, Machguth H, Maussion F and Pandit A 2019 A consensus estimate for the ice thickness distribution of all glaciers on Earth *Nat. Geosci.* **12** 168–73

- Giorgi F and Gutowski W J 2015 Regional dynamical downscaling and the CORDEX initiative *Annu. Rev. Environ. Resour.* **40** 467–90
- Grabherr G, Gottfried M and Pauli H 2010 Climate change impacts in alpine environments *Geogr. Compass* **4** 1133–53
- Gutierrez R A, Junquas C, Armijos E, Sörensson A A and Espinoza J-C 2024 Performance of regional climate model precipitation simulations over the terrain-complex andes-amazon transition region *J. Geophys. Res. Atmos.* **129** e2023JD038618
- Hardy D R, Vuille M and Bradley R S 2003 Variability of snow accumulation and isotopic composition on Nevado Sajama, Bolivia *J. Geophys. Res. Atmos.* **108**
- Hu Z, Guo Q, Li S, Piao S, Knapp A K, Ciais P, Li X and Yu G 2018 Shifts in the dynamics of productivity signal ecosystem state transitions at the biome-scale *Ecol. Lett.* **21** 1457–66
- Hugonnet R et al 2021 Accelerated global glacier mass loss in the early twenty-first century *Nature* **592** 726–31
- Jacobsen D and Dangles O 2017 *Ecology of High Altitude Waters* (Oxford University Press)
- Khamis K, Hannah D M, Clarvis M H, Brown L E, Castella E and Milner A M 2014 Alpine aquatic ecosystem conservation policy in a changing climate *Environ. Sci. Policy* **43** 39–55
- Körner C, Fajardo A and Hiltbrunner E 2023 Biogeographic implications of plant stature and microclimate in cold regions *Commun. Biol.* **6** 1–3
- Leyk S et al 2019 The spatial allocation of population: a review of large-scale gridded population data products and their fitness for use *Earth Syst. Sci. Data* **11** 1385–409
- Lopes R P, Scherer C S, Pereira J C and Dillenburg S R 2023 Paleoenvironmental changes in the Brazilian Pampa based on carbon and oxygen stable isotope analysis of Pleistocene camelid tooth enamel *J. Quat. Sci.* **38** 702–18
- Luo D, Hu Z, Dai L, Hou G, Di K, Liang M, Cao R and Zeng X 2023 An overall consistent increase of global aridity in 1970–2018 *J. Geogr. Sci.* **33** 449–63
- Madrigal-Martínez S and Miralles I García J L 2019 Land-change dynamics and ecosystem service trends across the central high-Andean Puna *Sci. Rep.* **9** 9688
- Malpede M and Percoco M 2023 Aridification, precipitations and crop productivity: evidence from the aridity index *Eur. Rev. Agric. Econ.* **50** 978–1012
- Masiokas M H et al 2020 A review of the current state and recent changes of the Andean cryosphere *Front. Earth Sci.* **8** 99
- Masson-Delmotte V et al (eds) 2021 *Climate Change 2021: The Physical Science Basis. Contribution of Working Group I to the Sixth Assessment Report of the Intergovernmental Panel on Climate Change* (Cambridge University Press) (<https://doi.org/10.1017/9781009157896>)
- McKeen T et al 2023a Gridded population estimates for 40 countries in Latin America and the Caribbean using official population estimates, version 1.0 (University of Southampton) (<https://doi.org/10.5258/SOTON/WP00755>)
- McKeen T et al 2023b High-resolution gridded population datasets for Latin America and the Caribbean using official statistics *Sci. Data* **10** 436
- Millan R, Mouginot J, Rabatel A and Morlighem M 2022 Ice velocity and thickness of the world's glaciers *Nat. Geosci.* **15** 124–9
- Moraes R M and Sarmiento J 2018 *Biodiversity in Bolivia Global Biodiversity* (Apple Academic Press)
- Moura M M et al 2019 Relation of El Niño and La Niña phenomena to precipitation, evapotranspiration and temperature in the Amazon basin *Sci. Total Environ.* **651** 1639–51
- Otto M, Scherer D and Richters J 2011 Hydrological differentiation and spatial distribution of high altitude wetlands in a semi-arid Andean region derived from satellite data *Hydrol. Earth Syst. Sci.* **15** 1713–27
- Pomeroy J W, Marsh P and Gray D M 1997 Application of a distributed blowing snow model to the Arctic *Hydrol. Process.* **11** 1451–64
- Rabatel A et al 2013 Current state of glaciers in the tropical Andes: a multi-century perspective on glacier evolution and climate change *The Cryosphere* **7** 81–102
- Rabatel A, Ducasse E, Ramseyer V and Millan R 2023 State and fate of glaciers in the val veny (Mont-Blanc Range, Italy): contribution of optical satellite products *J. Alp. Res. [Rev. de Geogr. Alp.]* **111**–2
- Rahbek C, Borregaard M K, Colwell R K, Dalsgaard B, Holt B G, Morueta-Holme N, Nogues-Bravo D, Whittaker R J and Fjeldsø J 2019 Humboldt's enigma: what causes global patterns of mountain biodiversity? *Science* **365** 1108–13
- RGI-Consortium 2017 Randolph glacier inventory—a dataset of global glacier outlines: version 6.0 *Technical Report* (Global Land Ice Measurements from Space)
- Rockström J, Falkenmark M, Karlberg L, Hoff H, Rost S and Gerten D 2009 Future water availability for global food production: the potential of green water for increasing resilience to global change *Water Resour. Res.* **45**
- Sierra-Almeida A, Cavieres L A and Bravo L A 2010 Freezing resistance of high-elevation plant species is not related to their height or growth-form in the Central Chilean Andes *Environ. Exp. Bot.* **69** 273–8
- Sturm M, Holmgren J and Liston G E 1995 A seasonal snow cover classification system for local to global applications *J. Clim.* **8** 1261–83
- Taylor K E, Stouffer R J and Meehl G A 2012 An overview of CMIP5 and the experiment design *Bull. Am. Meteorol. Soc.* **93** 485–98
- Testolin R et al 2021 Global patterns and drivers of alpine plant species richness *Glob. Ecol. Biogeogr.* **30** 1218–31
- Thrasher B, Wang W, Michaelis A, Melton F, Lee T and Nemani R 2022 NASA global daily downscaled projections, CMIP6 *Sci. Data* **9** 262
- Toledo O, Palazzi E, Cely Toro I M and Mortarini L 2022 Comparison of elevation-dependent warming and its drivers in the tropical and subtropical Andes *Clim. Dyn.* **58** 3057–74
- Tovar C et al 2022 Understanding climate change impacts on biome and plant distributions in the Andes: challenges and opportunities *J. Biogeogr.* **49** 1420–42
- United Nations Environment Programme 1997 World atlas of desertification: second edition (available at: <https://wedocs.unep.org/xmlui/handle/20.500.11822/30300>)
- Zhang R, Tian D, Chen H Y H, Seabloom E W, Han G, Wang S, Yu G, Li Z and Niu S 2022 Biodiversity alleviates the decrease of grassland multifunctionality under grazing disturbance: a global meta-analysis *Glob. Ecol. Biogeogr.* **31** 155–67
- Zhao W, Kou Y, Wang X, Wu Y, Bing H, Liu Q and Soininen J 2020 Broad-scale distribution of diazotrophic communities is driven more by aridity index and temperature than by soil properties across various forests *Glob. Ecol. Biogeogr.* **29** 2119–30
- Zomer R J, Xu J and Trabucco A 2022 Version 3 of the global aridity index and potential evapotranspiration database *Sci. Data* **9** 409